Characterizing the N2O isotopomer behavior of two N-disturbed soils using natural abundance and isotopic labelling techniques

Emily Stuchiner[1] and Joseph C. von Fischer[1]

[1]Colorado State University

November 26, 2022

Abstract

Nitrous oxide (N_2O), a potent greenhouse gas that contributes significantly to climate change, is emitted mostly from soils by a suite of microbial metabolic pathways that are nontrivial to identify, and subsequently, to manage. Using either natural abundance or enriched stable isotope methods has aided in identifying microbial sources of N_2O, but each approach has limitations. Here, we conducted a novel pairing of natural abundance and enriched assays on two dissimilar soils, hypothesizing this pairing would better constrain microbial sources of N_2O. We incubated paired natural abundance and enriched soils from a corn agroecosystem and a subalpine forest in the laboratory at 10-95% soil saturation for 28 hr. The natural abundance method measured intramolecular site preference (SP) from emitted N_2O, whereas the enriched method measured emitted $^{15}N_2O$ from soils amended with ^{15}N-labelled substrate. The isotopic composition of emitted N_2O was measured using a laser-based N_2O isotopic analyzer, yielding three key findings. First, isotopic signatures from natural abundance and enriched N_2O generally agreed in interpretation. Second, our novel pairing of isotopic methodologies refined understanding of microbial N-transformations in drier agricultural soil. In the 50% saturation agricultural soil, nitrification might have been deemed an important process based on SP alone, but enrichment helped reveal that its contribution to N_2O emissions was minor. Finally, we quantified, to our knowledge for the first time, persistent (>50%) β-position-specific enrichment in emitted $^{15}N_2O$, which is far in excess of SP-level fractionation expectations. This counter-intuitive enrichment pattern raises the possibility of previously unrecognized N-transformations in these soils.

Hosted file

`supplemental information_final.docx` available at https://authorea.com/users/554383/articles/605592-characterizing-the-n2o-isotopomer-behavior-of-two-n-disturbed-soils-using-natural-abundance-and-isotopic-labelling-techniques

Characterizing the N_2O isotopomer behavior of two N-disturbed soils using natural abundance and isotopic labelling techniques

E. R. Stuchiner[1,2] and J. C. von Fischer[1,2]

[1]Graduate Degree Program in Ecology, Colorado State University, Fort Collins, CO

[2]Department of Biology, Colorado State University, Fort Collins, CO

Corresponding author: Emily Stuchiner (emily.stuchiner@colostate.edu)

Key Points:

- Pairing natural abundance and enriched stable isotope methods improves confidence in disentangling microbial sources of N_2O
- N_2O isotopic signatures from natural abundance or ^{15}N-enriched soils generally agreed in interpretation of microbial source process
- Consistent position-specific enrichment patterns from emitted enriched N_2O may reveal previously unrecognized soil N-transformations

Abstract

Nitrous oxide (N_2O), a potent greenhouse gas that contributes significantly to climate change, is emitted mostly from soils by a suite of microbial metabolic pathways that are nontrivial to identify, and subsequently, to manage. Using either natural abundance or enriched stable isotope methods has aided in identifying microbial sources of N_2O, but each approach has limitations. Here, we conducted a novel pairing of natural abundance and enriched assays on two dissimilar soils, hypothesizing this pairing would better constrain microbial sources of N_2O. We incubated paired natural abundance and enriched soils from a corn agroecosystem and a subalpine forest in the laboratory at 10-95% soil saturation for 28 hr. The natural abundance method measured intramolecular site preference (SP) from emitted N_2O, whereas the enriched method measured emitted $^{15}N_2O$ from soils amended with ^{15}N-labelled substrate. The isotopic composition of emitted N_2O was measured using a laser-based N_2O isotopic analyzer, yielding three key findings. First, isotopic signatures from natural abundance and enriched N_2O generally agreed in interpretation. Second, our novel pairing of isotopic methodologies refined understanding of microbial N-transformations in drier agricultural soil. In the 50% saturation agricultural soil, nitrification might have been deemed an important process based on SP alone, but enrichment helped reveal that its contribution to N_2O emissions was minor. Finally, we quantified, to our knowledge for the first time, persistent (>50%) β-position-specific enrichment in emitted $^{15}N_2O$, which is far in excess of SP-level fractionation expectations. This counter-intuitive enrichment pattern raises the possibility of previously unrecognized N-transformations in these soils.

Plain Language Summary

Microbes in soils respire the greenhouse gas nitrous oxide (N_2O), which contributes to global warming. Respiration is a chemical reaction comparable to breathing. When environmental conditions like air temperature or soil moisture change, microbes respire N_2O differently, but often in ways we can neither easily anticipate nor identify. Fortunately, microbes all respire some naturally "heavy" forms of N_2O molecules, called heavy isotopes. Microbes emit different amounts of heavy isotopes when they respire different ways. To combat global warming, we aimed to better understand microbial N_2O emissions by bringing together two methods to measure heavy N_2O isotopes: natural abundance and labelling. Natural abundance measures the heavy isotopes microbes naturally emit, and labelling is when scientists feed microbes isotopically heavy food to trace how they respire the heavy isotopes. We put soils in sealed jars for 28 hours, and then measured the emitted heavy N_2O from each method with a specialized beam of laser-light. We better identified how microbes emitted N_2O when we used natural abundance *and* labelling at the same time. And so, two methods are better than one. Moving forward, we can use both methods to more precisely identify how microbes emit N_2O and better control global warming.

1. Introduction

Nitrous oxide (N_2O) is a far more potent greenhouse gas (GHG) than other biogenic GHGs (Ravishinkara et al. 2009, Cias et al. 2013). On a per molecule basis, N_2O has a warming potential 298x greater than carbon dioxide (CO_2) and 34x greater than methane (CH_4) (Alvarez et al. 2012, Rector et al. 2018). This is problematic because the atmospheric N_2O concentration has risen an unprecedented 20% since the Industrial Revolution began (Ciais et al. 2013). Microbial metabolism of synthetic and manure-based nitrogen (N) fertilizers in agricultural soils are largely responsible for this sharp rise in atmospheric N_2O (Davidson 2009, Park et al. 2012, Smith 2017). In fact, approximately 70% of N_2O is emitted from soils, but primarily from soils with an abundant inorganic N supply, hereafter classified as "N-disturbed" soils. In N-disturbed soils, N supply exceeds soil carbon (C) availability, which typically manifests in heightened microbial N metabolism and excess N_2O emissions (Davidson 2009).

Multiple microbial metabolic pathways can generate N_2O, and so it can be difficult to identify the process(es) responsible for emissions (Snider 2011, Zhang et al. 2016, Ibraim et al. 2018, Wong et al. 2020). Microbes can emit N_2O via nitrification, dissimilatory nitrate reduction to ammonium (DNRA), denitrification (bacterial and fungal), nitrifier-denitrification, co-denitrification, and anaerobic ammonia oxidation (anammox; Butterbach-Bahl et al. 2013). However, identifying the microbial source process(es) responsible for emissions is particularly challenging because each process is sensitive to a variety of spatially and temporally variable factors such as soil physical and chemical properties, climate, moisture, availability of N substrate, and microbial community composition and activity (Jenny 1980, Wrage et al. 2004, Park et al. 2011, Toyoda et al. 2015, van Groenigen et al. 2015, Congreves et al. 2019, Denk et al. 2019). To further complicate matters, processes can co-occur, sometimes even being performed by the same soil microbe (Wen et al. 2016, Sanford et al. 2012). Taken together, this

consort of variables makes it difficult to comprehensively identify the microbial processes responsible for N_2O emissions over space and time. To manage rising N_2O levels, we must be able to better identify which microbial pathways are responsible for emissions, especially in N-disturbed soils.

Stable isotopes have proven central to understanding the biochemical source processes of N_2O (Baggs 2008, Baggs 2011, Snider 2011, Snider et al. 2015, Hu et al. 2015, Yu et al. 2020). Both natural abundance and enriched methods have been used to quantify these sources (Perez et al. 2006, Ostrom and Ostrom 2012, Screiber et al. 2012, Ostrom and Ostrom 2017, Yamamoto et al. 2017). Isotopic enrichment has proved a reliable and robust method for partitioning among the better-studied N_2O-generating processes, nitrification and denitrification (Wrage et al. 2004, Mathieu et al. 2006, Wagner-Riddle et al. 2008, Russow et al. 2009). By amending a given soil with isotopically labelled $^{15}NH_4^+$ or $^{15}NO_3^-$, researchers can reveal when nitrification or denitrification dominates by tracing the emitted enriched N_2O back to the enriched substrate. However, ^{15}N additions are somewhat limiting in that they only partition between the two broad classes of processes.

In contrast, a number of studies have now characterized the natural abundance intramolecular distribution of ^{15}N in the N_2O molecule to delineate among multiple N_2O-producing processes (Sutka et al. 2006, Chen et al. 2016). Like many biochemical transformations, stable isotope fractionation occurs during N_2O production (Menyailo and Hungate 2006, Vieten et al. 2007, Lewicka-Szczebak et al. 2015, Snider et al. 2015). This causes differential accumulation of heavy N in either the central, α-position N, or the terminal, β-position N, in the linear N_2O molecule ($^{\beta}N={}^{\alpha}N=O$, Yoshida and Toyoda 2000). The intramolecular distribution, or difference in $\delta^{15}N$ between $\delta^{15}N^{\alpha}$ and $\delta^{15}N^{\beta}$ isotopomers, is termed

site preference (SP, Yoshida and Toyoda 2000). Since the early 2000s, a number of pure culture, lab, and field studies have shown that many N_2O-generating processes reliably yield consistent SP values (Toyoda et al. 2005, Sutka et al. 2006, Well et al. 2006, Perez et al. 2006, Baggs 2008, Park et al., 2011, Snider 2011, Maeda et al., 2015). To date, researchers have used SP to disentangle nitrification via ammonium oxidizing Archaea (AOA) or ammonium oxidizing bacteria (AOB), fungal vs. bacterial denitrification, and nitrifier denitrification (Wrage et al. 2004, Sutka et al. 2006, Wu et al. 2016, Wrage-Mönnig et al. 2018, Rohe et al. 2020). However, there are disagreements in the literature about the robustness of this method for multiple reasons. First, interlaboratory calibration for N_2O isotopic standards remains an ongoing issue (Mohn et al. 2014, Ostrom and Ostrom 2017, Ostrom et al. 2018, Harris et al. 2020). Second, SP values have been reported to overlap among very different source processes (e.g., nitrification and fungal denitrification, Decock and Six 2013, Xia et al. 2013, Hu et al. 2015, Wenk et al. 2016, Yamamoto et al. 2017, Yu et al. 2020). And third, $N_2O \rightarrow N_2$ reduction during denitrification enriches $\delta^{15}N^{\alpha}$ and can thus confound SP values (Koster et al. 2013, Mohn et al. 2014, Ostrom and Ostrom 2017, Lewicka-Szczebak et al. 2020, Stuchiner et al. 2020). To overcome the individual limitations of enriched and natural abundance studies, we hypothesize that pairing both methods on the same soils could enable better partitioning among N_2O-generating source processes.

Here, we used natural abundance and enriched methods on the same soils to characterize the agreement between the two methods. To our knowledge, this is the first study to deploy the two methods jointly for comparison. We performed natural abundance and enriched laboratory incubations on soils from two N-disturbed sites: a corn agroecosystem with varying levels of N-fertilization and irrigation, and a subalpine forest impacted by ~30 years of atmospheric N

pollution. We also manipulated soil moisture in each incubation to promote diverse N_2O-generating microbial metabolic pathways. By incubating different N-disturbed soils under both natural abundance and isotopically enriched conditions, we aimed to reveal gaps in our understanding about these isotopic approaches, and better understand the microbial N-transformations occurring in different soils. If effective, these methods in conjunction could be another strategy for constraining the global N_2O budget.

2. Materials and Methods

2.1 Field sampling and soil characterization

2.1.1 Site descriptions

We collected soils from two contrasting, N-disturbed ecosystems in Colorado: a corn field and a subalpine forest. Soil properties and treatments for each site are summarized Table 1.

Table 1. Properties and treatment descriptions (as applicable) for all sites. Percent soil organic C (SOC) and soil organic N (SON), and microbial biomass C and N were measured in June 2018. Growing season irrigation or N application was averaged across all the same agricultural treatments plots, and the subalpine values are for the entire watershed surrounding that subalpine environment. The n-value for soil treatment corresponds to the number of plots that samples were collected from. The n-values for all other measurements correspond to the number of technical replicates from each bulked soil sample. Error bars represent ± one SE from the mean.

Site	Soil treatment	Abbreviated soil name	Irrigation (mm/ growing season)	Total N application rate (kg/ha/yr)	% SOC	% SON	Microbial Biomass C (µg C/g dry soil)	Microbial Biomass N (µg N/g dry soil)
Agriculture	High N High Water (n = 4)	HNHW	497	266	1.21 (± 0.162) (n = 4)	0.077 (± 0.003) (n = 4)	9.00 (± 0.600) (n = 4)	0.918 (± 0.340) (n = 4)
Agriculture	High N Low Water (n = 3)	HNLW	441	270	1.36 (± 0.036) (n = 4)	0.098 (± 0.017) (n = 4)	5.92 (± 1.08) (n = 4)	0.301 (± 0.081) (n = 4)
Agriculture	Low N High Water (n = 4)	LNHW	497	172	1.28 (± 0.060) (n = 4)	0.093 (± 0.002) (n = 4)	6.59 (± 1.75) (n = 4)	0.554 (± 0.390) (n = 4)
Agriculture	Low N Low Water (n = 3)	LNLW	441	154	1.47 (± 0.090) (n = 4)	0.102 (± 0.004) (n = 4)	11.5 (±2.51) (n = 4)	0.934 (± 0.320) (n = 4)
Subalpine	None (n = 4)	Subalpine	N/A	3-3.5	7.82 (± 1.20) (n = 4)	0.355 (± 0.086) (n = 4)	18.2 (± 3.16) (n = 3)	1.37 (± 0.490) (n = 3)

Agricultural site

We collected soil from the Limited Irrigation Research Farm (LIRF) located north of Greeley, Colorado (described in detail in Zhang and Yemoto 2018). In 2016, experimental treatments were applied across plots that measured approximately 6 x 20 m. These treatments manipulated soil irrigation and fertilizer N to assess the impact on corn crop yield (detailed in Table 1). The experimental design used 14 fully randomized treatment blocks with high or low irrigation rates, and high or low additions of urea and NO_3^- fertilizer. Thus, our treatments included: high N high water (HNHW), high N low water (HNLW), low N high water (LNHW), and low N low water (LNLW).

The high and low irrigation treatments provided crops with 100 and 65% of evapotranspiration (ET) met during the late vegetative and maturation growth stages. The high and low N additions were 250 and 130 kg/ha and were applied as a combination of liquid urea and NO_3^- in the irrigation water, which resulted in some discrepancies in the amount of fertilizer applied to plots, depending on HW or LW appointment. Liquid urea was applied in ~22 kg/ha drip fertigation aliquots throughout the vegetative growth stages (N. Flynn, *pers comm*).

Subalpine site

The Loch Vale Watershed (LVWS) is located in Rocky Mountain National Park (RMNP) on the eastern edge of the Front Range in Colorado, USA, between 3100 and 4000m elevation (described in detail in Heath and Baron 2014). LVWS is subjected to atmospheric N deposition due to easterly winds carrying inorganic N from agricultural, vehicle, and industrial sources along the Colorado Front Range into the park. The N falls primarily as wet deposition (Baron et al. 2000). The LVWS receives ~3-3.5 kg/ha/y of wet N deposition, which has previously been found to alter ecosystem processes (Baron et al. 2000; Booth et al. 2016; Oleksy et al. 2020). The

watershed receives ~105 cm of precipitation per year, with ~50 cm falling in the summer months (Heath and Baron 2014).

We collected soils from the subalpine forest at ~3200 m, sampling from four randomly selected GPS coordinates where the conditions appeared undisturbed by human foot traffic. No sampling was conducted on the long-term N fertilization plots (Boot et al. 2016).

2.1.2 Soil collection and analyses

All soils were collected either in the second week of June 2018 or the third week of July 2018. Soils were collected using a 5cm-diameter soil auger to a depth of ~20 cm. Six cores were collected randomly throughout each sampling plot and bulked into gallon Ziploc bags. Bags were placed on ice in the field to minimize microbial activity, and then refrigerated at 4 C upon return to the lab. Within 24 hr after sampling, soils were sieved to 2mm and homogenized by treatment. Ziploc bags containing the processed soil were frozen at -18 C. All incubations and analyses were performed within three months after soils were collected.

Prior to freezing soils, we performed KCl extractions and calculated soil gravimetric water content. To quantify soil NH_4^+ and NO_3^- levels, we mixed 10 g soil subsamples with 50 mL 2M KCl, and they were shaken at 250 rpm for 1 hr, settled overnight, and then gravity filtered. Extracts were frozen and thereafter analyzed colorimetrically using an Alpkem FIA wet chemistry system (O.I. Analytical, College Station TX). We determined gravimetric water content by drying subsamples to a constant weight in a 105 C oven.

After soils had been frozen, we measured soil pH, soil organic C and N (SOC and SON), and soil microbial biomass C and N (MBC and MBN). We created slurries of 1:10 soil to DI water and then measured soil pH with a benchtop meter (Thermo Scientific Orion Star™ A211 Benchtop pH Meter, Waltham, MA, USA). Frozen soil subsamples were dried in a 60 C oven

and then ground for SOC and SON analysis with a LECO Tru-Spec CN analyzer (Leco Corp., St. Joseph, MI, USA). Microbial biomass was extracted from 20 g frozen soil subsamples in 100 mL 0.5M K_2SO_4, and then solubilized in 1% chloroform. MBC and MBN were measured using a Shimadzu Total Organic Carbon analyzer that also measures ON (Shimadzu Scientific Instruments, Wood Dale, IL, USA). MBC and MBN were calculated as the differences between 1% chloroform slurry C or N and the extractable OC or ON concentration. Extraction efficiency was corrected at kEC = 0.45 and kEN = 0.46 (Zeglin et al. 2013). SOC, SON, MBC, and MBN were only measured for soils collected in June 2018.

Frozen soils were overnight shipped on ice to Ward Laboratories Inc. (Kearney, NE, USA), where soil phospholipid fatty acids (PLFAs) were extracted, saponified, and methylated to form fatty acid methyl esters (FAMEs) as in Allison et al. 2007. FAMEs were then identified and quantified using a capillary gas chromatograph. Ward Laboratories summed individual FAMEs into the following functional groups: Gram + bacteria, Gram – bacteria, arbuscular mycorrhizal fungi, saprophytes, protozoa, and undifferentiated using methods as in Allison et al. 2007, and afterwards we estimated total fungi:bacteria ratios for each soil.

2.1.3 Determination of soil saturation

To manipulate soil moisture, we first determined the soil maximum water holding capacity (WHC). By sieving our soils, we broke down all soil pore structures, so % water-filled pore space (WFPS), which is used to calculate field capacity, was of no use here (Farquharson and Baldock 2008). Instead, we thawed subsamples of the frozen, field-moist soil and amended them with DI water until fully saturated, or at maximum WHC. Then, we dried samples to a constant weight in a 105 C oven and calculated saturated water content by dividing the g water in the subsample by the subsample dry soil mass.

To determine the desired soil saturation for a given sample, we multiplied the desired percent soil saturation by the saturated water content. Then, to determine the g of water to add to a given sample, we multiplied the difference between the subsample GWC and desired soil saturation by the g soil incubated.

2.1.4 Comparison of soil properties at two time points

For our experiments, we incubated soils under isotopically enriched conditions and at natural abundance. Due to the limited volume of soil we were permitted to collect in June 2018, we collected more soil in July 2018. As such, the isotopically enriched incubations were performed on June soils, and only on the subalpine soil and the HNHW soil from the agricultural site. Dissimilarly, the natural abundance incubations were performed on all the soil types (see Table 1) we collected in July.

To account for differences in soil properties from June to July that could impact microbial activities, we compared all measured soil properties for the soils used in enriched and natural abundance incubations (subalpine and HNHW) with t-tests. Since the other agricultural soils were not used in June, we did not compare how their properties changed from June to July.

2.2 Soil incubations

2.2.1 Soil amendments and incubation setup

Soils were separated into two treatment groups: those amended with isotopically enriched substrate and those held at natural abundance. For all incubations, the frozen soil equivalent of 50g of dry soil (this varied by site and soil treatment) was weighed into 0.5 L Ball jars and refrigerated overnight to thaw. Prior to amendment, all soils were removed from the refrigerator and warmed slowly to room temperature to reduce disruption of microbial cellular membranes (Boot et al. 2016).

Soils that were isotopically enriched were amended with 98 AP excess $^{15}NH_4Cl$ or $Na^{15}NO_3$ at an application rate of less than 3% soil NH_4^+ or NO_3^- to prevent fertilization. The stable isotope tracer was dissolved in DI water and pipetted over the soils at a constant application rate, and then additional DI water was distributed by pipette over the soils to bring soils to the desired saturations (10-95% soil saturation). After all liquid was added to a given soil, it was mixed thoroughly to ensure sufficient distribution of stable isotope tracer and homogeneous saturation.

Soils that were held at natural abundance were brought to desired saturations either via additions of DI water or through air drying on ice to reduce microbial activity. For the soils that needed to be air dried, they were weighed periodically (~every 10 min) to track moisture loss until the desired dryness was reached.

After soils were brought to their desired saturation and amended with tracer (if applicable), jars were sealed for incubation (Diagram 1). It is methodologically challenging to balance the need for a small headspace (thus maximizing final N_2O concentration) with the need to remove large volumes of air for isotopic analysis from a hard-sided incubation jar (more details in Section 3). We compromised with a design that included a 0.5L jar and a 1L gas bag connected to the jar headspace. The jar lid was drilled to contain two ports with Swagelok bulkhead fittings. One fitting vented to ¼ in Tygon tubing with a two-way stopcock for gas sampling. The other fitting vented to a luerslip that could be fitted with a two-way stopcock attached to a 1 L Tedlar gas bag.

Diagram 1. Incubation jar-gas bag apparatus. Panel **a** is a conceptual model of the apparatus, and panel **b** shows a photograph of the apparatus.

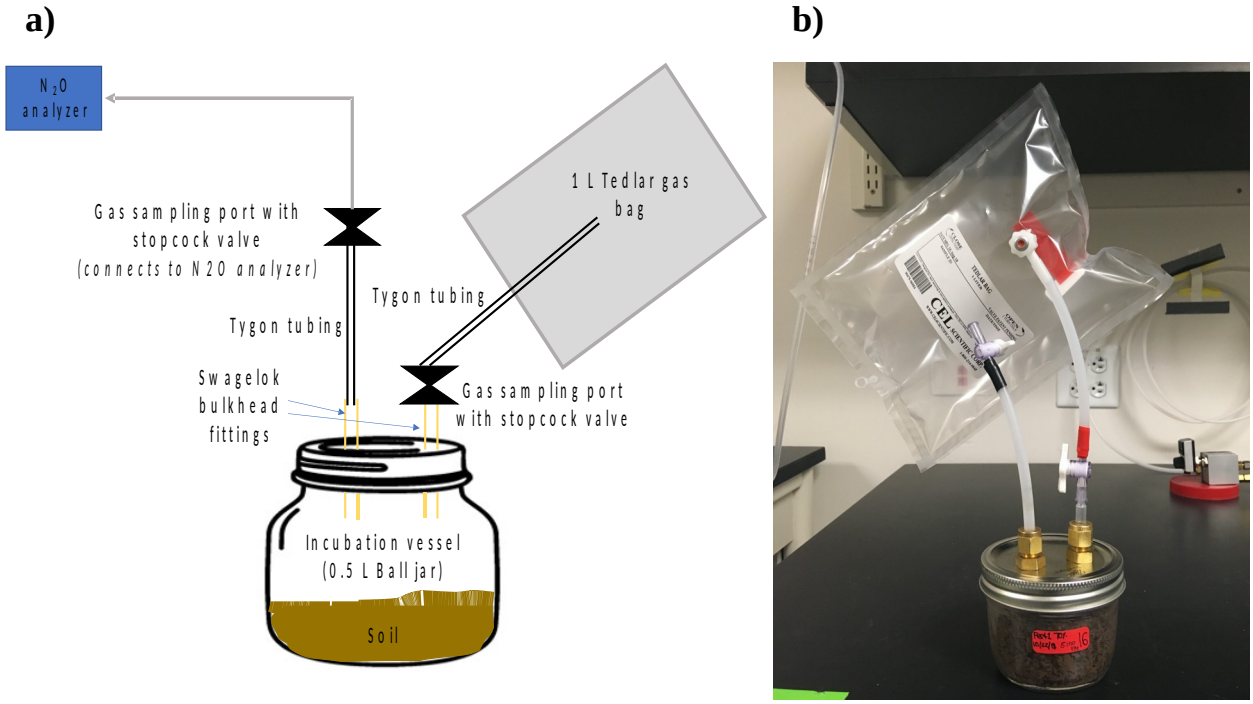

At the outset of the incubation, we flushed all jars and filled associated gas bags from a cylinder of medical-grade compressed air to provide a uniform starting gas background (Airgas Industries, etc.). Soils were incubated on in an interior lab countertop, at approximately 24 C for 28 hr. At the end of the incubation period, we mixed the jar and gas bag air with a 60 mL syringe to homogenize the headspaces. At the time of sampling, we connected the gas analyzer instrument system directly to the headspace-gas bag apparatus. Removal of jar headspace air thus emptied the gas bag and jar headspaces together, keeping the jar air pressure at atmospheric levels.

2.2.2 Measurements of N_2O concentration and isotopic compositions

After 28 hours, incubation vessels were attached to our laser-based Los Gatos Research (LGR) N_2O isotopic analyzer. Gas was sampled from each incubation vessel for 12-15 minutes

(or until the N_2O concentration stabilized). Samples were attached to the analyzer upstream of a Nafion-Carbosorb-Silica gel scrubbing system to remove CO_2, H_2O vapor, and VOCs from the sampling stream. This measure is taken to minimize the optical peak-broadening effects inherent to laser-based analyzers, as these effects can decrease the accuracy of reported N_2O concentrations. For further details, see Stuchiner et al. (2020).

We previously described the instrumental determination of N_2O concentration and isotopic composition (Stuchiner et al. 2020). Briefly, our analyzer measures concentrations of N_2O ($^{14}N^{14}N^{16}O$) and all its isotopomers ($^{14}N^{15}N^{16}O$, $^{15}N^{14}N^{16}O$, and $^{14}N^{14}N^{18}O$) using cavity enhanced laser absorption spectroscopy (Los Gatos Research N_2O Isotopic Analyzer model 914–0027; ABB-Los Gatos Research, Mountain View, CA, USA) in a continuous flow-through system without pre-concentration of the incoming gas.

All raw concentration data for each sample was exported to Excel (version 16.46) where it was trimmed to include only the N_2O and isotopomer concentrations after readings had stabilized. N_2O concentration and each isotopomer was calibrated using the model described in Stuchiner et al. (2020), and then converted to δ notation. We calculated the δ values using standard notation and the $^{15}N/^{14}N$ ratio of atmospheric N_2 (0.0036765) or the $^{18}O/^{16}O$ in VSMOW (0.0020052). All δ values are in ‰. The $\delta^{18}O$ values are reported in the Supplemental Information (Figure S1).

Equations 1-3 can be used to determine the δ values for the N_2O isotopomers:

$$(1)\ \delta N^{\alpha} = ¿¿¿¿$$

$$(2)\ \delta N^{\beta} = ¿¿¿¿$$

$$(3)\ \delta O = ¿¿¿¿$$

And to determine SP we used Equation 4:

$$(4)\ SP = \delta^{15}N^{\alpha} - \delta^{15}N^{\beta}$$

At low N_2O concentrations the SP data was consistently unreliable or out of the biologically plausible range, so we did not use any SP data from those incubations. Despite generally good precision and accuracy at N_2O concentrations above 2 ppm, we have observed that the instrument periodically reported SP values that were far outside of the plausible range (Stuchiner et al. 2020). According to Hu et al. (2015), this plausible range goes from -30 to 50‰, but we decided to extend the range from -40 to 65‰ because there is uncertainty surrounding the "true" biologically plausible SP range owing to ambiguity in isotopomer calibration and analytical precision (Ostrom and Ostrom 2017, Stuchiner et al. 2020). Thus, we excluded 10 of the 59 samples included in our analysis, where they reported biologically implausible SP values. The complete SP dataset is presented in Table S1. The majority of these implausible values were associated with relatively low N_2O concentrations (Figure S3).

2.2.3 Leak test of incubation apparatus

A separate test was performed to assess the gastight seals of the incubation apparati used in this experiment (Diagram 1). Twelve incubation apparati were filled with zero-grade air (80:20 N_2:O_2 blend, Airgas Industries) as described in Section 2.2.1 and injected with 1 mL of 99 atom percent (AP) $^{15}N^{15}N\,O$ using a 3 mL syringe, raising the N_2O concentration to ~500ppb and the $\delta^{15}N^{bulk}$ to ~6300‰. Six apparati were sampled for N_2O and its isotopomer concentrations 1 hr after preparation (T0) and the remaining six apparati were sampled 48 hr after preparation (T48). All samples were taken on our LGR N_2O isotopic analyzer. Change in total N_2O concentration was not significant, while change in ^{15}N enriched N_2O was < 2.3% for all isotopomers.

2.3 Data analysis

All raw data was collected and collated in Excel, and then all statistical analyses were performed in RStudio (version 4.0.2 (2020-06-22) -- "Taking Off Again" © 2020 The R Foundation for Statistical Computing). Differences among inherent soil properties and treatment effects were examined using ANOVAs and t-tests. Residuals were examined for departure from normality, and all N_2O production data for the enriched incubations were log-transformed to meet assumptions of normality in residuals. All predicted N_2O production data for the natural abundance incubations were also log-transformed to meet assumptions of normality in residuals.

The logistic regressions used to predict N_2O production rates were fitted in RStudio with the package `dr4pl`.

3. Results

3.1 Soil properties

Soils from the agricultural and subalpine sites differed sharply in biogeochemical properties. The June soils are summarized in Table 2. There were notable differences in most soil properties between the HNHW and subalpine June soils ($p < 0.05$ in all cases), excluding fungi:bacteria ratios, which were not significantly different.

Table 2. Biogeochemical properties of HNHW and subalpine soils collected in June 2018. The n-value for each measurement corresponds to the number of technical replicates within each bulked soil treatment. Error bars represent ± one SE from the mean.

Soil treatment	NO_3^- (µg N/g dry soil)	NH_4^+ (µg N/g dry soil)	Fungi:Bacteria (% fungi/% bacteria)	Soil pH
HNHW	80.3 (± 6.51) (n = 10)	3.03 (± 1.09) (n = 10)	0.193 (± 0.035) (n = 4)	7.90 (± 0.06) (n = 8)
Subalpine	1.06 (±0.420) (n = 9)	5.35 (± 1.29) (n =9)	0.192 (± 0.030) (n = 3)	5.14 (± 0.08) (n = 9)

The July soils are summarized in Table 3. The soil NO_3^- concentrations were notably higher in all agricultural soils compared to the subalpine soil ($p < 0.001$). Interestingly, pairwise comparisons illustrate that only the HNHW soil had a significantly higher NO_3^- concentration

compared to the other agricultural soils ($p < 0.05$ in all cases). The other treatments of the agriculture soil did not substantially influence NO_3^- concentration, regardless of HN or LN appointment. This is likely due to high concentrations of dissolved NO_3^- in the irrigation water.

Table 3. Biogeochemical properties of agricultural and subalpine soils collected in July 2018. The n-value for each measurement corresponds to the number of technical replicates within each bulked soil treatment. Error bars represent ± one SE from the mean.

Soil treatment	NO_3^- (µg N/g dry soil)	NH_4^+ (µg N/g dry soil)	Fungi:Bacteria (% fungi/% bacteria)	Soil pH
HNHW	77.9 (± 4.74) (n = 12)	1.80 (± 0.23) (n = 12)	0.142 (± 0.008) (n = 4)	8.15 (± 0.03) (n = 8)
HNLW	19.5 (± 6.19) (n = 9)	2.82 (± 0.04) (n = 9)	0.177 (± 0.014) (n = 3)	8.12 (± 0.04) (n = 6)
LNHW	13.3 (± 1.31) (n = 12)	1.80 (± 0.14) (n = 12)	0.188 (± 0.023) (n = 4)	8.16 (± 0.05) (n = 8)
LNLW	8.51 (± 0.74) (n = 9)	2.07 (± 0.07) (n = 9)	0.183 (± 0.013) (n = 3)	8.32 (± 0.04) (n = 6)
Subalpine	0.500 (±0.13) (n = 18)	5.11 (± 0.74) (n =18)	0.267 (± 0.020) (n = 8)	4.72 (± 0.04) (n = 18)

Pairwise comparisons also demonstrate that all agricultural soils had significantly less NH_4^+ compared to the subalpine soil ($p < 0.001$ in all cases), but none of the agricultural soils differed in NH_4^+ concentration.

There were some differences in fungi:bacteria ratios for soils sampled in July. While there were no differences in fungi:bacteria within the agricultural soils, the HNHW soil had a significantly lower fungi:bacteria ratio from the subalpine soil ($p = 0.0016$), and the HNHW, LNHW, and LNLW soils had borderline significantly lower fungi:bacteria ratios compared to the subalpine soil ($p = 0.045$, $p = 0.056$, $p = 0.071$, respectively).

Soil pH was slightly basic for all agricultural soils and slightly acidic for the subalpine soil ($p < 0.001$).

Finally, we compared the HNHW and subalpine soil properties from June to July. We determined no significant differences in soil NO_3^-, NH_4^+, or fungi:bacteria within each soil from June to July ($p > 0.05$ in all cases). However, both soils differed in pH from June to July, with the HNHW soil becoming more basic ($p = 0.005$) and the subalpine soil becoming more acidic ($p < 0.001$).

3.2 Soils held at natural abundance

3.2.1 N_2O production rate in natural abundance soils

N_2O production rates showed a clear threshold response to variation in soil moisture (Figure 1). At low soil moistures (10-50% soil saturation), N_2O production rate was relatively low and constant. However, at approximately 60% soil saturation, we observed a marked increase in N_2O production rate (Figure 1). We fit the following four-parameter logistic model to the data to characterize these response curves (Equation 5):

$$(5)\ y = d + \frac{a-d}{1+\left(\frac{x}{c}\right)^b}$$

Where a is the minimum value, b is the slope of the line, c is the inflection point on the line (halfway point between a and d), and d is the maximum value. Each of these values correspond to a biologically relevant N_2O production parameter (Table 3).

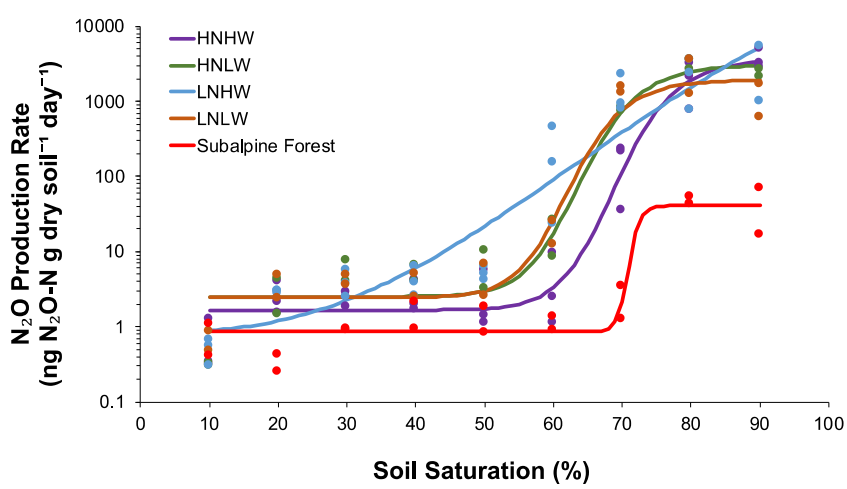

Figure 1. N_2O production rates for all soils that were held from 10 to 90% soil saturation. Data points correspond to observed production rate values and fitted lines are modelled predictions of N_2O production rate for all soils. All fits were modelled using logistic regressions. For the

observed data, n = 27 for HNHW, n = 26 for LNHW, and n = 18 in all other cases. *Note the log-scaled y-axis*.

The results of these regressions are in Table 2. All logistic fits were strong (R^2 range from 0.88 to 0.94). These fits allowed us to compare the mean water content where soil N_2O production rate flipped from low production rates to high production rates (Table 4). For most agricultural soils, the transition point was at approximately 60% soil saturation, and for the subalpine soil the transition point was at approximately 70% soil saturation (Figure 1).

Table 4. Summary of fit data comparing N_2O production rate data to estimated N_2O production rate data using logistic regressions. The R^2 values correspond to simple linear regressions comparing real production rate data to estimated production rate data, and the p-values correspond to each R^2 value. The values a-d correspond to the parameters estimated from each logistic regression. Parameter values occur from Equation 5. *Note the parameters and R^2 values result from log-transformed N_2O production rate data.*

Site	Treatment	Sample size (n)	R^2	Minimum N_2O production rate (a)	Slope (b)	Soil saturation transition point (c)	Maximum N_2O production rate (d)
Agricultural							
	HNHW	27	0.94	0.511	16.3	69.2	8.22
	HNLW	18	0.92	0.924	15.3	64.0	8.03
	LNHW	26	0.90	-0.170	2.65	83.5	15.8
	LNLW	18	0.94	0.906	15.6	62.3	7.58
Subalpine forest							
	Subalpine	18	0.88	-0.155	89.8	70.9	3.71

It is worth noting that the soil saturation transition point is notably higher for the LNHW soil. The poorer model fit for this soil is likely due to one very high observed N_2O production rate value that pulls the modeled values up, which is which the LNHW curve does not flatten at high soil moistures, like the other curves do.

3.2.2. Intramolecular site preference (SP) at natural abundance

Across all soils, intramolecular SP generally decreased as percent soil saturation increased (Figure 2). Linear regression across all data points was significant (p = 0.01) with an R^2 of 0.25. However, at 90% saturation, SP increased for HNLW, LNLW, and the subalpine soil (Figure 2). Across all soil saturations, HNHW tended to have more enriched SP values than other

soils. While there is only data for the subalpine soil starting at 60% soil saturation, this soil also tended to have more enriched SP values. Across all saturations, HNLW, HNLW, and LNLW soils reported SP values between the HNHW and subalpine SP endpoints (Figure 2).

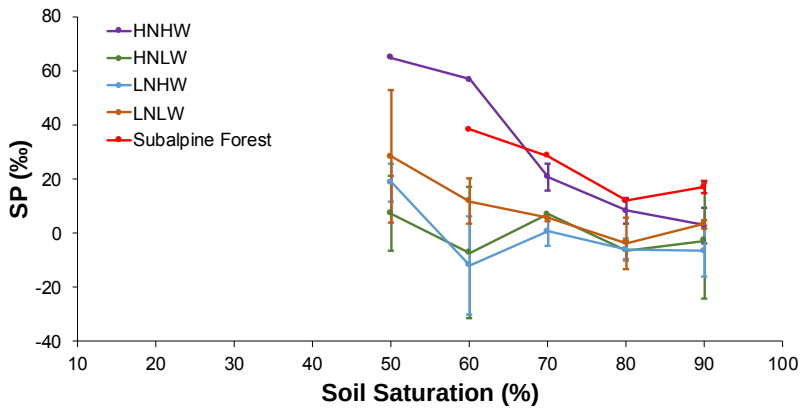

Figure 2. Intramolecular SP for all soils from 50-90% soil saturation. SP values were only used from this soil saturation range because values from lower soil saturations were deemed unreliable or not biologically realistic. Error bars represent ± one SE from the mean. *Note not all data points have error bars, as multiple soils have n = 1 at certain soil saturations*. All sample size information is summarized in Table S2.

While all soils followed the same general patterns with increasing saturation, there was a substantial degree of variability among SP values at each saturation level (Figure 2). At 50% soil saturation, SP ranged from 65‰ for HNHW to 7‰ for HNLW. Interestingly, as saturation increased, the degree of difference among SP values decreased, however soils deviated from this trend at 90% saturation (Figure 2). At this soil saturation the range of values widened. The subalpine soil had an SP of 17‰, whereas the LNHW soil had an SP of -7‰.

Together, the similar magnitudes and directions of SP values across soils indicate that microbes were likely performing similar N-transformations at each saturation level. However, variation among values within each saturation level could indicate soil-specific differences in microbial behavior. These distinctions may be able to help better elucidate finer-scale differences in microbial metabolism across soils.

3.3 Isotopically amended soils

3.3.1 N_2O production rate in isotopically amended soils

There was no difference in N_2O production rate within each soil saturation level. This indicates that there was no treatment effect from the $^{15}NO_3^-$ vs. $^{15}NH_4^+$ amendments (Figure 3).

N_2O production rate was highest in the 90% saturation agricultural soils (1650 and 1928 ng N_2O-N/g dry soil/day from soils amended with $^{15}NH_4^+$ and $^{15}NO_3^-$, respectively), but markedly decreased in the 50% saturation soils (3.87 and 3.78 ng N_2O-N/g dry soil/day from soils amended with $^{15}NH_4^+$ and $^{15}NO_3^-$, respectively; Figure 3).

The subalpine soil had intermediate N_2O production rates at both saturations (Figure 3). N_2O production rate was higher in the 85% saturated soils (451 and 528 ng N_2O-N/g dry soil/day from soils amended with $^{15}NH_4^+$ and $^{15}NO_3^-$, respectively), and lower in the 95% saturated soils (168 and 147 ng N_2O-N/g dry soil/day from soils amended with $^{15}NH_4^+$ and $^{15}NO_3^-$, respectively), suggesting that $N_2O \rightarrow N_2$ reduction could be an important process in the wettest subalpine soils.

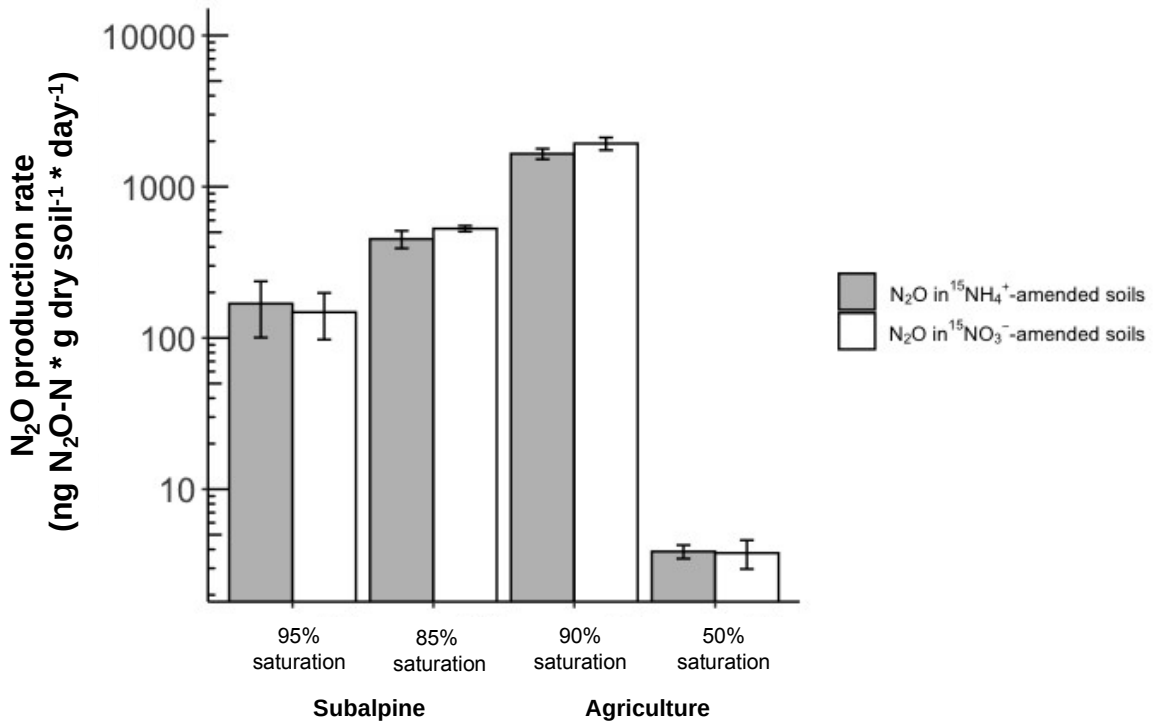

Figure 3. N_2O production rates from agricultural and subalpine soils across all soil moisture and isotopic enrichment treatments. In all cases n = 4 except n = 3 for the $^{15}NO_3^-$-amended 50% saturation agricultural soil. Error bars represent ± one SE from the mean. *Note the log scale y-axis.*

3.3.2 Tracing $^{15}N^{bulk}$ signatures to source partition among microbial processes

Across all soil saturations, the majority of ^{15}N-label was emitted from soils amended with $^{15}NO_3^-$ compared to soils amended with $^{15}NH_4^+$ (Figure 4; $p < 0.001$). In the $^{15}NO_3^-$-amended soils, the largest $^{15}N^{bulk}$ signature (AP) was emitted from the 90% saturation agricultural soil, the smallest $^{15}N^{bulk}$ signature was emitted from the 50% saturation agricultural soil, and intermediate between those two were the subalpine soils, with the 95% saturation soil emitting a greater $^{15}N^{bulk}$ signature than the 85% saturation subalpine soil (Figure 4a).

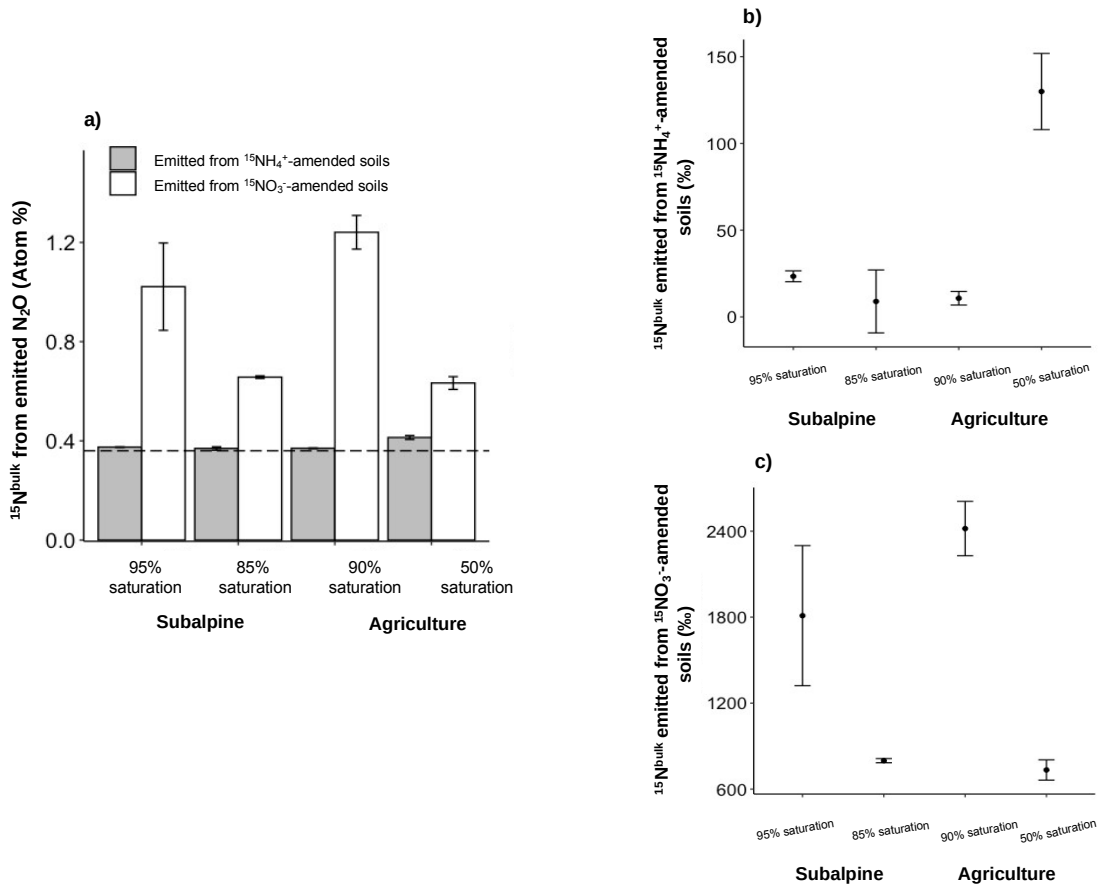

Figure 4. *Panel **a***: $^{15}N_2O^{bulk}$ in AP emitted from $^{15}NH_4^+$ or $^{15}NO_3^-$ amended soils. *Panel **b**:* $\delta^{15}N_2O^{bulk}$ emitted from $^{15}NH_4^+$ amended soils. *Panel **c**:* $\delta^{15}N_2O^{bulk}$ emitted from $^{15}NO_3^-$amended soils. In all cases n = 4 except n = 3 for the $^{15}NO_3^-$-amended 50% saturation agricultural soil. Error bars represent ± one SE from the mean. The dashed horizontal line in Panel **a** indicates the AP threshold for isotopic enrichment above natural abundance (0.36 %).

In the $^{15}NH_4^+$-amended soils, the $^{15}N^{bulk}$ signatures for the two subalpine soils and the 90% saturation agricultural soil were mostly homogenous and concordant with natural abundance isotopic enrichment (3 to 45‰; Figure 4c). In contrast, the $^{15}N^{bulk}$ signature for the 50% saturation soil was significantly more enriched than the other $^{15}NH_4^+$-amended soils ($p < 0.001$), and reported a mean AP and δ value substantially above ambient (0.41% and 130‰, respectively, Figure 4a, 4c). Because soils were amended with highly enriched substrate (99 AP excess $^{15}NH_4^+$), this indicates that NH_4^+ was not an important substrate for microbial processes in

three of the four soils at these moisture levels, but it was at least tractably used for microbial metabolism in the 50% saturation agricultural soil, albeit not appreciably (Figure 4c).

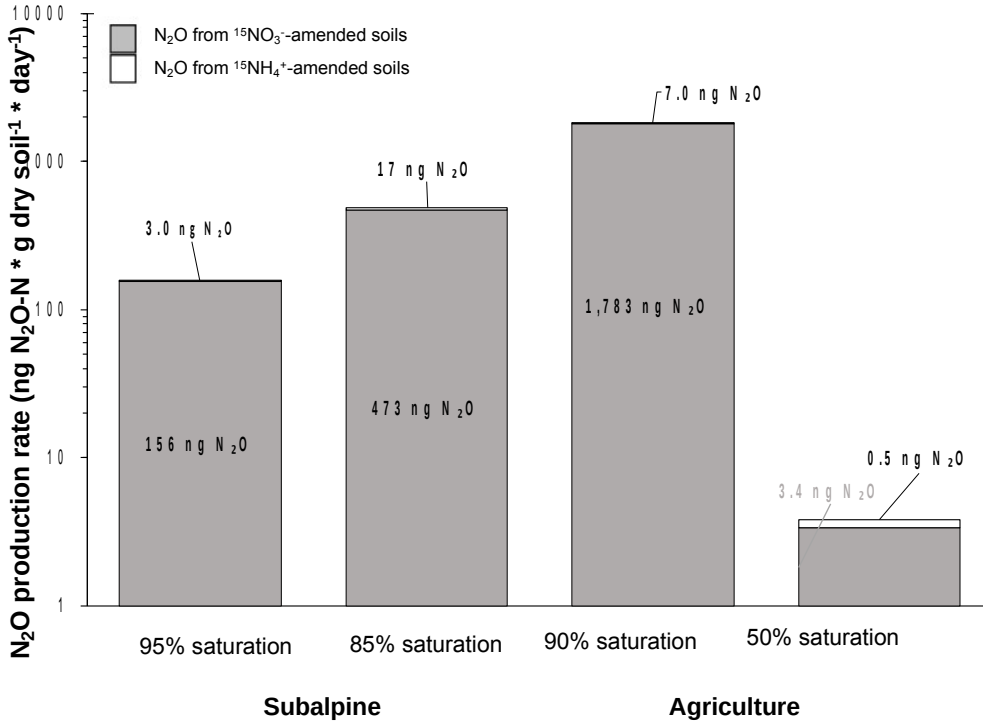

Figure 5. N_2O production rates partitioned by NH_4^+-consuming vs. NO_3^-–consuming pathways. In most cases, the majority of emitted N_2O is generated from microbial NO_3^- use, although a detectable fraction of emitted N_2O is generated via microbial NH_4^+ use in the $^{15}NH_4^+$-amended 50% saturation agricultural soil. In all cases, n = 4, except n = 3 for the $^{15}NO_3^-$-amended 50% saturation agricultural soil. Error bars represent ± one SE from the mean.

We also calculated the total N_2O production rate for each soil partitioned by N_2O emitted from $^{15}NO_3^-$ or $^{15}NH_4^+$-amended soil. This analysis further illustrates that most emitted N_2O came from NO_3^- transformations, but a minute fraction of emitted N_2O came from NH_4^+ transformations (Figure 5). Together, Figures 4 and 5 show that 1) the majority of emitted N_2O was generated via NO_3^- transformations, 2) there is some variability in $^{15}N^{bulk}$ signatures and N_2O production rate among the $^{15}NO_3^-$-amended soils, and 3) a small, but non-neglible fraction of N_2O was emitted from NH_4^+ transformations. While this is not surprising, given that the soils are

all held at different saturations, this variability suggests that microbial activity likely differs among the soils.

3.3.3 Isotopic enrichment in the $\delta^{15}N^{\alpha}$ vs. $\delta^{15}N^{\beta}$ position of the emitted N_2O

The location of isotopic enrichment (α-position or β-position) in the emitted N_2O varied among soils and by type of isotopic amendment. We chose to present this data by quantifying the percent of emitted N_2O enriched in the β-position ($^{15}N – N – O$) from each soil by calculating the atom percent enrichment (APE) in each isotopomer, using Equations 6 and 7, where $AP^{15}N^{x}$ is the $AP^{15}N^{\alpha}$ or $^{15}N^{\beta}$, and AP_{std} corresponds to the AP of $^{15}N/(^{15}N+^{14}N)$ in N_2-Air (i.e., 0.003663):

$$(6)\ APE \in \beta\ position = AP^{15}N^{\beta} - AP_{std}$$
$$APE \in \alpha\ position = AP^{15}N^{\alpha} - AP_{std}$$

$$(7)\ Fraction\ of\ enriched\ 15N \in \beta\ position = \frac{APE\ \beta\ position}{APE\ \beta\ position + APE\ \alpha\ position}$$

On the converse, the fraction of N_2O enriched in the α-position ($N – ^{15}N – O$) from each soil would be 1 - fraction β-position enrichment.

The majority of the emitted enriched N_2O derived from the $^{15}NO_3^-$-amended soils, so we chose to focus on those soils for our analysis of α and β-position enrichment (Figure 4). Information about the α and β-position enrichment from the $^{15}NH_4^+$-amended soils is available in the Supplemental Information (Figure S2).

In the $^{15}NO_3^-$-amended soils, the 90% saturation agricultural soil emitted significantly more N_2O enriched in the β-position than the other three soils ($p < 0.001$; Figure 6) as characterized by highly negative SP values (Table S3). Conversely, neither the two subalpine soils nor the 50% saturation agricultural soil emitted significantly different amounts of N_2O enriched in the β-position. The 90% saturation agricultural soil emitted 60% of β-position-

enriched N_2O, whereas the 50% saturation agricultural soil, the 95% saturation subalpine soil, and the 85% saturation subalpine soil emitted 54, 54, and 55% β-position-enriched N_2O, respectively (Figure 6). Meaning, the 90% saturation agricultural soil was the least enriched in the α-position, whereas the other three soils had comparable amounts of α-position enrichment. However, one-sample t-tests compared each soil's fraction of emitted $^{15}N^{\beta}$ to 50%; all soils emitted significantly more than 50% β-position-enriched N_2O ($p < 0.05$ in all cases).

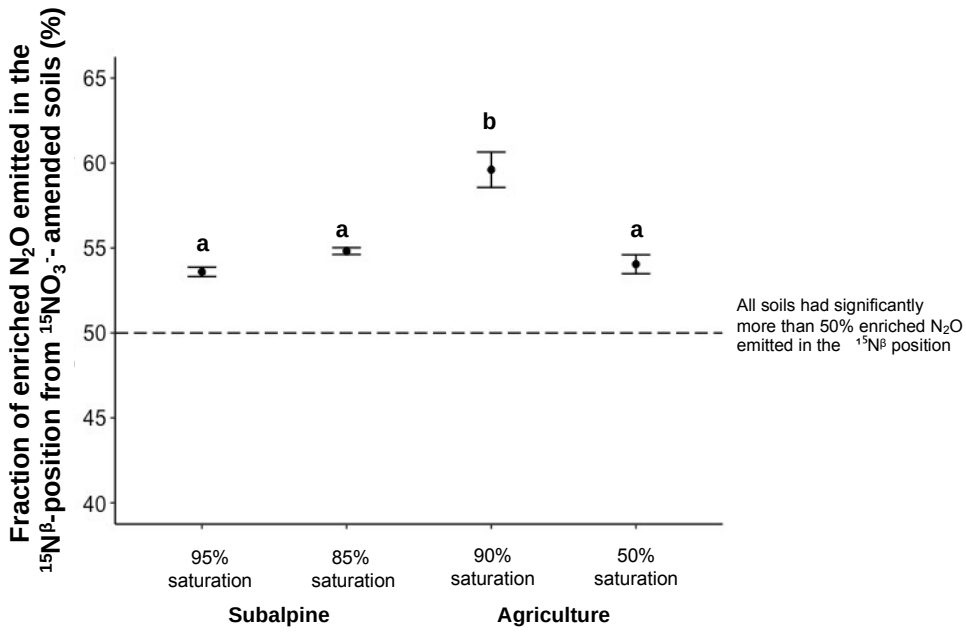

Figure 6. Percent of emitted N_2O enriched in the β-position (^{15}N—N—O) from each $^{15}NO_3^-$-amended soil. In all cases, n = 4, except n = 3 for the $^{15}NO_3^-$-amended 50% saturation agricultural soil. Bars represent a 95% CI around the mean. For all soils, significantly more than half of the enriched N_2O emitted was enriched in the β-position (all percentages significantly above 50% dotted line). Different letters illustrate significantly different means. *Note: the percent β-position enriched N_2O was only considered for the $^{15}NO_3^-$-amended soils because those soils emitted almost all the isotopically enriched N_2O.*

4. Discussion

By incubating N-disturbed soils under both natural abundance and enriched conditions, we sought to better understand how well these isotopic methods align, and which microbial source processes were driving N_2O emissions. To our knowledge, this is the first study to pair enriched and natural abundance N stable isotope methods directly to examine N_2O production

pathways. Methodologically, we acknowledge that this study has some limitations, but it has allowed us to make some interesting insights into microbial N_2O-generating activity. In particular, there is generally good agreement between natural abundance and enriched approaches, with some interesting departures. This work also led to new, unique observations of position-specific enriched isotopomers, which both raise questions about biogeochemical pathways and suggest a future tool for tracing pathways of N_2O emission.

4.1 Modelling N_2O production rate

The general response of our natural abundance incubated soils to variation in soil moisture is consistent with previous studies, such that N_2O production rates showed a strong threshold behavior with much higher rates of emissions at higher soil moisture (Figure 1; Parton et al. 1996, Del Grosso et al. 2000, Li and Aber 2000, Parton et al. 2001, Ni et al. 2011, Taylor et al. 2017, Ji et al. 2018, Song et al. 2019,). While the specific logistic regression we applied is not important, this type of model fit allows us to extract useful parameters about N_2O production capacity from these diverse soils (Table 4).

Our findings are consistent with classic interpretations of microbial N_2O metabolism, such as the hole-in-the-pipe (HIP) and the "anaerobic balloon," wherein the transition from aerobic to anerobic metabolism is consistent with a shift from nitrification to denitrification, and this is largely dictated by soil WFPS (Firestone and Davidson 1989, Li and Aber 2000, Butterbach-Bahl et al. 2013). While we used percent soil saturation, not WFPS, our findings align with Davidson (1993), who illustrates that from WFPS 60 to ~85%, most of the N-gas flux is emitted as N_2O. This likely also helps to explain why the modelled N_2O production rate stabilized for most of our soils at 90% saturation (Figure 1). However, it is worth noting that the maximum N_2O production rates differed quite a bit among soil treatments, which is likely

modulated by other variables that effect the N_2O:N_2 emission ratio, such as soil NO_3^- or OC (Firestone and Davidson 1989; Figure 1). Overall, the patterns we observed support our approach of manipulating soil moisture to induce diverse N_2O production pathways and supports our exploration of N_2O stable isotope responses.

4.2 Patterns in natural abundance SP

The trend we observed for SP in natural abundance incubations (Fig. 2) was clear and may also suggest finer-scale differences in soil microbial behavior. The observed decline in SP as soils became more saturated is consistent with literature SP values that indicate a transition from nitrification to denitrification as soils get wetter (Bergstermann et al. 2011, Denk et al. 2017, Congreves et al. 2019, Ding et al. 2019). It is worth noting that in some cases n = 1 or 2 replicates per treatment as a consequence of instrument errors leading to biologically implausible SP values (Stuchiner et al. 2020). Despite the small sample size, the pattern we observe showing a transition from larger to smaller SP with increasing soil moisture is coherent, both within and among soils (Figure 2).

That said, there is some nuance in the SP patterns that might provide insights into soil microbial N_2O metabolism. We observed a SP of 65‰ for the 50% saturation HNHW soil (Figure 2). Although higher SP values in drier soils are often consistent with nitrification, this value falls above the reported range for nitrification of 9 to 46‰ (Löscher et al. 2012, Hu et al. 2015, Denk et al. 2017, Ding et al. 2019, Lewicka-Szczebak et al. 2020). Higher SP values can be indicative of fungal denitrification (~20 to 45‰), but previous research suggests fungal denitrification is unlikely to be dominant at this dry soil moisture level, and there were no large soil aggregates to host fungal denitrification in our finely-seived soil (Hu et al. 2015, Maeda et al. 2015, Denk et al. 2017). Recently, Wong et al. (2020) reported similarly high SP values (83‰

± 25‰) in marine sediments and posit that multiple biotic and abiotic processes proceeding through multiple cycles could account for such enrichment. Additionally, it is also possible that a yet-identified SP, like that for DNRA, could be responsible for this isotopic signature, since DNRA has been reported in soils under drier conditions, where NO_3^- might be more bioavailable (Rütting et al. 2011, Schmidt et al. 2011, Zhang et al. 2015, Friedl et al. 2018).

We also see generally more enriched SP values for HNHW and subalpine soils across all saturations. In the subalpine soil, we were able to measure biologically plausible SP values starting at 60% saturation, when denitrification tends to become more important (Groffman 2012, Fang et al. 2015, Cardenas et al. 2017, Schlüter et al. 2019, Thilarkarathna and Hernandez-Ramirez 2021). Fungal denitrification could be responsible for more enriched SP values from the subalpine soil, as the subalpine soil had greater fungi:bacteria ratio than the other soils (Table 3). In contrast, the HNHW soil has the lowest fungi:bacteria ratio (Table 3). Thus, this pattern in HNHW soils support Wong et al.'s (2020) assertion that more enriched SP values are due to multiple processes co-occurring and proceeding through multiple cycles.

Lastly, we observed increases in SP in HNLW, LNLW, and the subalpine soil at 90% saturation (Figure 2). These increases support previous findings that SP increases as $N_2O \rightarrow N_2$ reduction becomes more important, which is typical in anoxic and more reducing conditions (Ostrom et al. 2010, Decock and Six 2013, Wu et al. 2016, Gaimster et al. 2018, Congreves et al. 2019).

In sum, these more subtle patterns in SP values suggest nuance in microbial N biogeochemistry and/or N_2O production pathways among soils that may have been missed if the assays had been of the more binary (i.e., nitrification vs. denitrification) ^{15}N isotope labeling type.

4.3 Isotopically enriched vs. natural abundance soils

In general, our use of ^{15}N-labelled inorganic substrates to create the enriched incubations corroborate our findings from natural abundance incubations. The wetter isotopically enriched soils (85, 90, and 95% saturation) emitted almost all N_2O from NO_3^- transformations, rather than from NH_4^+ transformations, suggesting denitrification (Figure 5). This aligns with the literature and our natural abundance findings (Figure 2): (1) previous studies show wetter, anoxic soils use NO_3^- as substrate for denitrification, (2) the classic range of bacterial denitrification SP goes from -11 to 0‰, and (3) our natural abundance HNHW and subalpine soils also show a general decrease in SP as they get wetter, indicating denitrification (Sutka et al. 2006, Butterbach-Bahl et al. 2013, Rohe et al. 2017, Congreves et al. 2019).

However, our isotopically enriched findings depart from dogmatic expectations at lower soil moisture, where the natural abundance data were likewise surprising. Specifically, while we expected the drier, more oxic 50% saturation HNHW soil to generate most of its N_2O from nitrification, the overwhelming majority of the N_2O came from $^{15}NO_3^-$ transformations (Figure 5, Russow et al. 2009, Ball et al. 2010, Parker and Schimel 2011, Wu et al. 2017, Tan et al. 2018). As noted in the previous section, the SP value was also unusually high (65‰) for this soil at 50% saturation. Together, these data suggest that co-occurring processes, such as DNRA and bacterial denitrification in anoxic microsites, could have given rise to the high $^{15}NO_3^-$ derived N_2O in the enriched soil and the uncharacteristically enriched SP in the natural abundance soil (Palacin-Lizarbe et al. 2019, Wong et al. 2020) Also, despite the one month time difference between enriched and natural abundance assays, it seems likely that the soils were behaving similarly, even after sieving the soil (hence breaking down natural soil pore structures) and creating artificial incubation conditions. For example, soil NH_4^+ and NO_3^- levels were very similar over time, and N_2O production rates were comparable (Tables 2 and 3, 3.6 vs. 2.8 ng

N_2O-N/g dry soil/day). Thus, although NO_3^- may not be the domainant source for N_2O in drier field conditions, it clearly was for this incubation, and the SP data suggest an interesting combination of processes leading to the N_2O emissions that we observed (Perez et al. 2006, Opdyke et al. 2009, Ostrom et al. 2010, Park et al. 2011). Clearly, the combined deployment of enriched and natural abundance methods created here a richer understanding of processes than would be generated by either approach alone.

4.4 Position-specific enrichment in isotopically labelled soils

By isotopically labelling soils with $^{15}NH_4^+$ or $^{15}NO_3^-$, we were able to determine, and report for the first time, position-specific ^{15}N-enrichment in the emitted N_2O from incubations. The majority of the emitted N_2O was from $^{15}NO_3^-$-amended soils, as we discussed above, but within that emitted N_2O, 54-60% of the ^{15}N appeared in the β-position (Figure 6). This begs the question: what can this strong degree of position-specific enrichment tell us? It would be ideal if isotopically enriched isotopomers and SP could be informative of microbial N_2O-generating pathways because these enriched signatures are far less ambiguous than natural abundance signatures (Wagner-Riddle et al. 2008; Zhang et al. 2015, Snider et al. 2017). Because most of the ^{15}N-enrichment in the emitted N_2O derived from the wetter (85, 90, and 95% saturation) $^{15}NO_3^-$-amended soils, bacterial denitrification was likely an important N_2O-generating pathway in these oxygen-poor soils (Figure 4; Parkin et al. 1987, Barnard et al. 2005, Baggs 2011, Krause et al. 2017, Smith 2017, Gaimster et al. 2018). At natural abundance, bacterial denitrification tends to correspond to low to negative SP, which aligns with the greater β-position enrichment we observed (SP = $\delta^{15}N^{\alpha} - \delta^{15}N^{\beta}$, so if $\delta^{15}N^{\beta}$ is bigger than $\delta^{15}N^{\alpha}$ SP will be smaller; Toyoda et al. 2005, Toyoda et al. 2015). However, our enriched samples showed strongly negative SP values

(e.g., in the negative hundreds, see Table S3), whereas at natural abundance SP does not typically get much lower than -30‰ (Wu et al. 2019; Hu et al. 2015).

Currently, we do not have an explanation for these strongly negative SP values from the enriched incubations, but three possibilities emerge. First, isotopically labelled enrichment may not scale proportionately with natural abundance enrichment. For example, Andriukonis and Gorokhova (2017) show that phytoplankton growth rate appreciably decreases as ^{15}N enrichment in the environment increases, likely due to the kinetic isotope effect (KIE). Although enrichment did not appear to impact N_2O production rate, as N_2O production rates between the enriched and natural abundance incubations are comparable, perhaps it impacted the isotopic composition of the emitted N_2O (Figure 1, Figure 3). Second, an inverse isotope effect, like Yang et al. (2014) observed, wherein the β-position N-atom binds more strongly to the active site on a denitrification enzyme, could have resulted in greater β-position enrichment in the emitted N_2O. Finally, this could be an indication of microbial N-transformations we have not yet discovered or do not yet fully understand biochemically. Future research should evaluate whether greater enrichment in the β-position occurs reliably under particular conditions. If strong patterns in position-specific enrichment are broadly observed, then this measure, like SP, could become another tool for understanding which microbial processes give rise to N_2O.

4.5 Concluding remarks

We sought to better understand how incubating the same soils under natural abundance and isotopically enriched conditions can better inform our ability to study microbial N_2O-generating processes. Our study yielded both confirmatory and novel insights. Our natural abundance incubations demonstrated that intramolecular SP decreases as soils transition from dry to wet, which generally aligns with nitrification to denitrification SP values from the

literature. Our isotopically enriched incubations yielded isotopic signatures that mostly agreed with the natural abundance isotopic signatures, which lends further credence to natural abundance SP methods. While we acknowledge that it can be logistically challenging for labs to perform natural abundance and isotopically enriched experiments in conjunction, our work demonstrates that it can result in more robust trust in N_2O isotopic datasets for determining microbial N_2O-generating pathways. As we improve our abilities to measure stable isotopes, it may become more useful to compare-contrast natural abundance and enriched signatures because natural abundance methods have the advantage of being less invasive, whereas enriched methods have the advantage of being, usually, less ambiguous.

Scientific research has made ample strides over the past ~30 years to improve our usage of stable isotopes for constraining the N_2O budget, but there remains need to continue to bolster confidence in these methods. Our study illustrates that pairing natural abundance and isotopically enriched soil incubations can reveal gaps in our understanding of microbial N-transformations and different isotopic methodologies. We encourage future studies to consider pairing these methods, and we also encourage researchers to assess position-specific N_2O enrichment, as this may be yet another emergent property of the N_2O molecule that can inform us about microbial N-metabolism.

Data Availability Statement

We have uploaded all finalized data to www.mountainscholar.org Accession number forthcoming.

Prepublication note: These data are embargoed, pending publication of this manuscript.

Acknowledgments, Samples, and Data

The authors declare no conflicts of interest in this work. All data supporting this manuscript are available via www.Mountainscholar.org. Due to limited remaining availability of frozen soil, the authors will instead be happy to assist interested researchers to obtain fresh samples from our local field sites, pending permission from the field site managers. We acknowledge financial

support from Colorado State University's Graduate Degree Program in Ecology and a grant from Environmental Defense Fund to JvF. We are grateful for lab and field assistance by Kelly Nelson and Tim Weinmann.

References

Allison, V. J., Z. Yermakov, R. M. Miller, J. D. Jastrow, and R. Matamala (2007), Assessing Soil Microbial Community Composition Across Landscapes: Do Surface Soils Reveal Patterns?, *Soil Sci. Soc. Am. J.*, *71*(3), 730–734, doi:10.2136/sssaj2006.0301n.

Alvarez, R. A., S. W. Pacala, J. J. Winebrake, W. L. Chameides, and S. P. Hamburg (2012), Greater focus needed on methane leakage from natural gas infrastructure, , (17), doi:10.1073/pnas.1202407109.

Andriukonis, E., and E. Gorokhova (2017), Kinetic 15N-isotope effects on algal growth, *Sci. Rep.*, *7*(March), 1–9, doi:10.1038/srep44181.

Baggs, E. M. (2008), A review of stable isotope techniques for N2O source partitioning in soils: recent progress, remaining challenges, and future considerations, *Rapid Commun. Mass Spectrom.*, *22*(22), 1664–1672, doi:10.1002/rcm.

Baggs, E. M. (2011), Soil microbial sources of nitrous oxide: Recent advances in knowledge, emerging challenges and future direction, *Curr. Opin. Environ. Sustain.*, *3*(5), 321–327, doi:10.1016/j.cosust.2011.08.011.

Ball, P. N., M. D. MacKenzie, T. H. DeLuca, and W. E. H. Montana (2010), Wildfire and Charcoal Enhance Nitrification and Ammonium-Oxidizing Bacterial Abundance in Dry Montane Forest Soils, *J. Environ. Qual.*, *39*(4), 1243–1253, doi:10.2134/jeq2009.0082.

Barnard, R., P. W. Leadley, and B. A. Hungate (2005), Global change, nitrification, and denitrification: A review, *Global Biogeochem. Cycles*, *19*(1), 1–13, doi:10.1029/2004GB002282.

Baron, J. S., H. M. Rueth, A. M. Wolfe, K. R. Nydick, E. J. Allstott, J. T. Minear, and B. Moraska (2000), Ecosystem responses to nitrogen deposition in the Colorado Front Range, *Ecosystems*, *3*(4), 352–368, doi:10.1007/s100210000032.

Bergstermann, A., L. Cárdenas, R. Bol, L. Gilliam, K. Goulding, A. Meijide, D. Scholefield, A. Vallejo, and R. Well (2011), Effect of antecedent soil moisture conditions on emissions and isotopologue distribution of N2O during denitrification, *Soil Biol. Biochem.*, *43*(2), 240–250, doi:10.1016/j.soilbio.2010.10.003.

Boot, C. M., E. K. Hall, K. Denef, and J. S. Baron (2016), Long-term reactive nitrogen loading alters soil carbon and microbial community properties in a subalpine forest ecosystem, *Soil Biol. Biochem.*, *92*, 211–220, doi:10.1016/j.soilbio.2015.10.002.

Butterbach-Bahl, K., E. M. Baggs, M. Dannenmann, R. Kiese, and S. Zechmeister-Boltenstern (2013), Nitrous oxide emissions from soils: how well do we understand the processes and their controls?, *Philos. Trans. R. Soc. London.*, *368*(1621), 20130122, doi:10.1098/rstb.2013.0122.

Cardenas, L. M., R. Bol, D. Lewicka-Szczebak, A. S. Gregory, G. P. Matthews, W. R. Whalley, T. H. Misselbrook, D. Scholefield, and R. Well (2017), Effect of soil saturation on denitrification in a grassland soil, *Biogeosciences Discuss.*, (1989), 1–51, doi:10.5194/bg-2016-556.

Chen, H., D. Williams, J. T. Walker, and W. Shi (2016), Probing the biological sources of soil N2O emissions by quantum cascade laser-based15N isotopocule analysis, *Soil Biol. Biochem.*, *100*, 175–181, doi:10.1016/j.soilbio.2016.06.015.

Ciais, P. et al. (2013), The physical science basis. Contribution of working group I to the fifth assessment report of the intergovernmental panel on climate change, *Chang. IPCC Clim.*, 465–570, doi:10.1017/CBO9781107415324.015.

Congreves, K. A., T. Phan, and R. E. Farrell (2019), A new look at an old concept: Using 15N2O isotopomers to understand the relationship between soil moisture and N2O production pathways, *Soil*, *5*(2), 265–274, doi:10.5194/soil-5-265-2019.

Davidson E.A. (1993) Soil Water Content and the Ratio of Nitrous Oxide to Nitric Oxide Emitted from Soil. In: Oremland R.S. (eds) Biogeochemistry of Global Change. Springer, Boston, MA. https://doi.org/10.1007/978-1-4615-2812-8_20.

Davidson, E. A. (2009), The contribution of manure and fertilizer nitrogen to atmospheric nitrous oxide since 1860, *Nat. Geosci.*, *2*(9), 659–662, doi:10.1038/ngeo608.

Decock, C., and J. Six (2013), How reliable is the intramolecular distribution of 15N in N2O to source partition N2O emitted from soil?, *Soil Biol. Biochem.*, *65*(2), 114–127, doi:10.1016/j.soilbio.2013.05.012.

Del Grosso, S. J., W. J. Parton, A. R. Mosier, D. S. Ojima, A. E. Kulmala, and S. Phongpan (2000), General model for N 2 O and N 2 gas emissions from soils due to dentrification, *Global Biogeochem. Cycles*, *14*(4), 1045–1060, doi:10.1029/1999GB001225.

Denk, T. R. A., J. Mohn, C. Decock, D. Lewicka-Szczebak, E. Harris, K. Butterbach-Bahl, R. Kiese, and B. Wolf (2017), The nitrogen cycle: A review of isotope effects and isotope modeling approaches, *Soil Biol. Biochem.*, *105*, 121–137, doi:10.1016/j.soilbio.2016.11.015.

Denk, T. R. A., D. Kraus, R. Kiese, K. Butterbach-Bahl, and B. Wolf (2019), Constraining N cycling in the ecosystem model LandscapeDNDC with the stable isotope model SIMONE, *Ecology*, *100*(5), 1–15, doi:10.1002/ecy.2675.

Ding, J., F. Fang, W. Lin, X. Qiang, C. Xu, L. Mao, Q. Li, X. Zhang, and Y. Li (2019), N 2 O emissions and source partitioning using stable isotopes under furrow and drip irrigation in vegetable field of North China, *Sci. Total Environ.*, *665*, 709–717, doi:10.1016/j.scitotenv.2019.02.053.

Fang, Y. et al. (2015), Microbial denitrification dominates nitrate losses from forest ecosystems, *Proc. Natl. Acad. Sci. U. S. A.*, *112*(5), 1470–1474, doi:10.1073/pnas.1416776112.

Farquharson, R., and J. Baldock (2008), Concepts in modelling N2O emissions from land use, *Plant Soil*, *309*(1–2), 147–167, doi:10.1007/s11104-007-9485-0.

Firestone, M. K., and E. A. Davidson (1989), Microbiologial Basis of NO and N20 production and consumption in soil, *Exch. Trace Gases between Terr. Ecosyst. Atmos.*, (January 1989), 7–21, doi:10.1017/CBO9781107415324.004.

Friedl, J., D. De Rosa, D. W. Rowlings, P. R. Grace, C. Müller, and C. Scheer (2018), Dissimilatory nitrate reduction to ammonium (DNRA), not denitrification dominates nitrate reduction in subtropical pasture soils upon rewetting, *Soil Biol. Biochem.*, *125*(May), 340–349, doi:10.1016/j.soilbio.2018.07.024.

Gaimster, H., M. Alston, D. J. Richardson, A. J. Gates, and G. Rowley (2018), Transcriptional and environmental control of bacterial denitrification and N2O emissions, *FEMS Microbiol. Lett.*, *365*(5), 1–8, doi:10.1093/femsle/fnx277.

Groffman, P. M. (2012), Terrestrial denitrification: Challenges and opportunities, *Ecol. Process.*, *1*(1), 1–11, doi:10.1186/2192-1709-1-11.

Harris, S. J. et al. (2020), N2O isotopocule measurements using laser spectroscopy: Analyzer characterization and intercomparison, *Atmos. Meas. Tech.*, *13*(5), 2797–2831, doi:10.5194/amt-13-2797-2020.

Heath, J., and J. S. Baron (2014), Climate, Not Atmospheric Deposition, Drives the Biogeochemical Mass-Balance of a Mountain Watershed, *Aquat. Geochemistry*, *20*(2–3), 167–181, doi:10.1007/s10498-013-9199-2.

Hu, H. W., D. Chen, and J. Z. He (2015), Microbial regulation of terrestrial nitrous oxide formation: Understanding the biological pathways for prediction of emission rates, *FEMS Microbiol. Rev.*, *39*(5), 729–749, doi:10.1093/femsre/fuv021.

Ibraim, E., E. Harris, S. Eyer, B. Tuzson, L. Emmenegger, J. Six, and J. Mohn (2018), Development of a field-deployable method for simultaneous, real-time measurements of the four most abundant N2O isotopocules, *Isotopes Environ. Health Stud.*, *54*(1), 1–15, doi:10.1080/10256016.2017.1345902.

Jenny H. (1980) Ecosystems and Soils. In: The Soil Resource. Ecological Studies (Analysis and Synthesis), vol 37. Springer, New York, NY. https://doi.org/10.1007/978-1-4612-6112-4_1.

Ji, Q., E. Buitenhuis, P. Suntharalingam, J. L. Sarmiento, and B. B. Ward (2018), Global Nitrous Oxide Production Determined by Oxygen Sensitivity of Nitrification and Denitrification, *Global Biogeochem. Cycles*, *32*(12), 1790–1802, doi:10.1029/2018GB005887.

Krause, H. M., C. Thonar, W. Eschenbach, R. Well, P. Mäder, S. Behrens, A. Kappler, and A. Gattinger (2017), Long term farming systems affect soils potential for N2O production and reduction processes under denitrifying conditions, *Soil Biol. Biochem.*, *114*, 31–41, doi:10.1016/j.soilbio.2017.06.025.

Köster, J. R., R. Well, B. Tuzson, R. Bol, K. Dittert, A. Giesemann, L. Emmenegger, A. Manninen, L. Cárdenas, and J. Mohn (2013), Novel laser spectroscopic technique for continuous analysis of N 2O isotopomers - Application and intercomparison with isotope ratio mass spectrometry, *Rapid Commun. Mass Spectrom.*, *27*(1), 216–222, doi:10.1002/rcm.6434.

Lewicka-Szczebak, D., R. Well, R. Bol, A. S. Gregory, G. P. Matthews, T. Misselbrook, W. R. Whalley, and L. M. Cardenas (2015), Isotope fractionation factors controlling isotopocule signatures of soil-emitted N2O produced by denitrification processes of various rates, *Rapid Commun. Mass Spectrom.*, *29*(3), 269–282, doi:10.1002/rcm.7102.

Lewicka-Szczebak, D., M. Piotr Lewicki, and R. Well (2020), N2O isotope approaches for source partitioning of N2O production and estimation of N2O reduction-validation with the 15N gas-flux method in laboratory and field studies, *Biogeosciences*, *17*(22), 5513–5537, doi:10.5194/bg-17-5513-2020.

Li, C., J. Aber, F. Stange, K. Butterbach-Bahl, and H. Papen (2000), A process-oriented model of N2O and NO emissions from forest soils: 1. Model development, *J. Geophys. Res. Atmos.*, *105*(D4), 4369–4384, doi:10.1029/1999JD900949.

Li, Q., F. Wang, Q. Yu, W. Yan, X. Li, and S. Lv (2019), Dominance of nitrous oxide production by nitrification and denitrification in the shallow Chaohu Lake, Eastern China: Insight from isotopic characteristics of dissolved nitrous oxide, *Environ. Pollut.*, *255*, 113212, doi:10.1016/j.envpol.2019.113212.

Löscher, C. R., A. Kock, M. Könneke, J. Laroche, H. W. Bange, and R. A. Schmitz (2012), Production of oceanic nitrous oxide by ammonia-oxidizing archaea, *Biogeosciences*, *9*(7), 2419–2429, doi:10.5194/bg-9-2419-2012.

Maeda, K., A. Spor, V. Edel-Hermann, C. Heraud, M.-C. Breuil, F. Bizouard, S. Toyoda, N. Yoshida, C. Steinberg, and L. Philippot (2015), N2O production, a widespread trait in fungi, *Sci. Rep.*, *5*(1), 9697, doi:10.1038/srep09697.

Mathieu, O., J. Lévêque, C. Hénault, M. J. Milloux, F. Bizouard, and F. Andreux (2006), Emissions and spatial variability of N2O, N2 and nitrous oxide mole fraction at the field scale, revealed with 15N isotopic techniques, *Soil Biol. Biochem.*, *38*(5), 941–951, doi:10.1016/j.soilbio.2005.08.010.

Menyailo, O. V., and B. A. Hungate (2006), Stable isotope discrimination during soil denitrification: Production and consumption of nitrous oxide, *Global Biogeochem. Cycles*, *20*(3), doi:10.1029/2005GB002527.

Mohn, J. et al. (2014), Interlaboratory assessment of nitrous oxide isotopomer analysis by isotope ratio mass spectrometry and laser spectroscopy: Current status and perspectives, *Rapid Commun. Mass Spectrom.*, *28*(18), 1995–2007, doi:10.1002/rcm.6982.

Ni, B. J., M. Ruscalleda, C. Pellicer-Nàcher, and B. F. Smets (2011), Modeling nitrous oxide production during biological nitrogen removal via nitrification and denitrification: Extensions to the general ASM models, *Environ. Sci. Technol.*, *45*(18), 7768–7776, doi:10.1021/es201489n.

Oleksy, I. A., W. S. Beck, R. W. Lammers, C. E. Steger, C. Wilson, K. Christianson, K. Vincent, G. Johnson, P. T. J. Johnson, and J. S. Baron (2020), The role of warm, dry summers and variation in snowpack on phytoplankton dynamics in mountain lakes, *Ecology*, *101*(10), 1–12, doi:10.1002/ecy.3132.

Opdyke, M. R., N. E. Ostrom, and P. H. Ostrom (2009), Evidence for the predominance of denitrification as a source of N 2O in temperate agricultural soils based on isotopologue measurements, *Global Biogeochem. Cycles*, *23*(4), 1–10, doi:10.1029/2009GB003523.

Ostrom, N. E., R. Sutka, P. H. Ostrom, A. S. Grandy, K. M. Huizinga, H. Gandhi, J. C. von Fischer, and G. P. Robertson (2010), Isotopologue data reveal bacterial denitrification as the primary source of N2O during a high flux event following cultivation of a native temperate grassland, *Soil Biol. Biochem.*, *42*(3), 499–506, doi:10.1016/j.soilbio.2009.12.003.

Ostrom, N. E., and P. H. Ostrom (2012), Handbook of Environmental Isotope Geochemistry, , doi:10.1007/978-3-642-10637-8.

Ostrom, N. E., and P. H. Ostrom (2017), Mining the isotopic complexity of nitrous oxide: a review of challenges and opportunities, *Biogeochemistry*, *132*(3), 359–372, doi:10.1007/s10533-017-0301-5.

Ostrom, N. E. et al. (2018), Preliminary assessment of stable nitrogen and oxygen isotopic composition of USGS51 and USGS52 nitrous oxide reference gases and perspectives on calibration needs, *Rapid Commun. Mass Spectrom.*, *32*(15), 1207–1214, doi:10.1002/rcm.8157.

Palacin-Lizarbe, C., L. Camarero, S. Hallin, C. M. Jones, J. Cáliz, E. O. Casamayor, and J. Catalan (2019), The DNRA-denitrification dichotomy differentiates nitrogen transformation pathways in mountain lake benthic habitats, *Front. Microbiol.*, *10*(JUN), 1–15, doi:10.3389/fmicb.2019.01229.

Park, S., T. Perez, K. A. Boering, S. E. Trumbore, J. Gil, S. Marquina, and S. C. Tyler (2011), Can N2O stable isotopes and isotopomers be useful tools to characterize sources and

microbial pathways of N2O production and consumption in tropical soils?, *Global Biogeochem. Cycles*, *25*(1), 1–16, doi:10.1029/2009GB003615.

Park, S. et al. (2012), Trends and seasonal cycles in the isotopic composition of nitrous oxide since 1940, *Nat. Geosci.*, *5*(4), 261–265, doi:10.1038/ngeo1421.

Parker, S. S., and J. P. Schimel (2011), Soil nitrogen availability and transformations differ between the summer and the growing season in a California grassland, *Appl. Soil Ecol.*, *48*(2), 185–192, doi:10.1016/j.apsoil.2011.03.007.

Parkin, T. B. (1987), Soil Microsites as a Source of Denitrification Variability, *Soil Sci. Soc. Am. J.*, *51*(5), 1194–1199, doi:10.2136/sssaj1987.03615995005100050019x.

Parton, W. J., A. R. Mosier, D. S. Ojima, D. W. Valentine, D. S. Schime, K. Weier, and A. E. Kulmala (1996), Generalized model for N2 and N2O production from nitrification and denitrification, *Global Biogeochem. Cycles*, *10*(3), 401–412, doi:10.1029/96GB01455.

Parton, W. J., E. a. Holland, S. J. Del Grosso, M. D. Hartman, R. E. Martin, a. R. Mosier, D. S. Ojima, and D. S. Schimel (2001), Generalized model for NOx and N2O emissions from soils, *J. Geophys. Res.*, *106*(2), 17403, doi:10.1029/2001JD900101.

Perez, T., D. Garcia-Montiel, S. E. Trumbore, S. C. Tyler, P. De Camargo, M. Moreira, M. Piccolo, and C. Cerri (2006), Nitrous oxide nitrification and denitrification 15N enrichment factors from Amazon forest soils, , *16*(6), 2153–2167.

Ravishankara, A. R., J. S. Daniel, and R. W. Portmann (2009), Nitrous oxide (N2O): The dominant ozone-depleting substance emitted in the 21st century, *Science (80-.).*, *326*(5949), 123–125, doi:10.1126/science.1176985.

Rector, C., K. R. Brye, J. Humphreys, R. J. Norman, E. E. Gbur, J. T. Hardke, C. Willett, and M. A. Evans-white (2018), Regional N 2 O emissions and global warming potential as affected by water management and rice cultivar on an Al fi sol in Arkansas , USA, *Geoderma Reg.*, *14*, e00170, doi:10.1016/j.geodrs.2018.e00170.

Rohe, L., R. Well, and D. Lewicka-Szczebak (2017), Use of oxygen isotopes to differentiate between nitrous oxide produced by fungi or bacteria during denitrification, *Rapid Commun. Mass Spectrom.*, *31*(16), 1297–1312, doi:10.1002/rcm.7909.

Rohe, L., T. Oppermann, R. Well, and M. A. Horn (2020), Nitrite induced transcription of p450nor during denitrification by Fusarium oxysporum correlates with the production of N2O with a high 15N site preference, *Soil Biol. Biochem.*, *151*(July), 108043, doi:10.1016/j.soilbio.2020.108043.

Russow, R., C. F. Stange, and H. U. Neue (2009), Role of nitrite and nitric oxide in the processes of nitrification and denitrification in soil: Results from 15N tracer experiments, *Soil Biol. Biochem.*, *41*(4), 785–795, doi:10.1016/j.soilbio.2009.01.017.

Rütting, T., P. Boeckx, C. Müller, and L. Klemedtsson (2011), Assessment of the importance of dissimilatory nitrate reduction to ammonium for the terrestrial nitrogen cycle, *Biogeosciences*, *8*(7), 1779–1791, doi:10.5194/bg-8-1779-2011.

Sanford, R. A. et al. (2012), Unexpected nondenitrifier nitrous oxide reductase gene diversity and abundance in soils, *Proc. Natl. Acad. Sci. U. S. A.*, *109*(48), 19709–19714, doi:10.1073/pnas.1211238109.

Schmidt, C. S., D. J. Richardson, and E. M. Baggs (2011), Constraining the conditions conducive to dissimilatory nitrate reduction to ammonium in temperate arable soils, *Soil Biol. Biochem.*, *43*(7), 1607–1611, doi:10.1016/j.soilbio.2011.02.015.

Smith, K. A. (2017), Changing views of nitrous oxide emissions from agricultural soil: key controlling processes and assessment at different spatial scales, *Eur. J. Soil Sci.*, *68*(2), 137–155, doi:10.1111/ejss.12409.

Schlüter, S., J. Zawallich, H. J. Vogel, and P. Dörsch (2019), Physical constraints for respiration in microbial hotspots in soil and their importance for denitrification, *Biogeosciences*, *16*(18), 3665–3675, doi:10.5194/bg-16-3665-2019.

Snider, D. M. (2011), A characterization of the controls of the nitrogen and oxygen isotope ratios of biologically-produced nitrous oxide and nitrate in soils, (Doctoral dissertation). Retrieved from UWSpace. (https://uwspace.uwaterloo.ca/bitstream/handle/10012/6053/Snider_David.pdf?sequence=1&isAllowed=y) Waterloo, Ontario, Canada: University of Waterloo.

Snider, D., K. Thompson, C. Wagner-Riddle, J. Spoelstra, and K. Dunfield (2015), Molecular techniques and stable isotope ratios at natural abundance give complementary inferences about N2O production pathways in an agricultural soil following a rainfall event, *Soil Biol. Biochem.*, *88*, 197–213, doi:10.1016/j.soilbio.2015.05.021.

Snider, D. M., C. Wagner-Riddle, and J. Spoelstra (2017), Stable Isotopes Reveal Rapid Cycling of Soil Nitrogen after Manure Application, *J. Environ. Qual.*, *46*(2), 261–271, doi:10.2134/jeq2016.07.0253.

Song, X., X. Ju, C. F. E. Topp, and R. M. Rees (2019), Oxygen Regulates Nitrous Oxide Production Directly in Agricultural Soils, *Environ. Sci. Technol.*, *53*(21), 12539–12547, doi:10.1021/acs.est.9b03089.

Stuchiner, E. R., Z. D. Weller, and J. C. Fischer (2020), An approach for calibrating laser−based N 2 O isotopic analyzers for soil biogeochemistry research , *Rapid Commun. Mass Spectrom.*, (June 2020), 1–14, doi:10.1002/rcm.8978.

Sutka, R. L., N. E. Ostrom, P. H. Ostrom, J. A. Breznak, H. Gandhi, A. J. Pitt, and F. Li (2006), Distinguishing Nitrous Oxide Production from Nitrification and Denitrification on the Basis of Isotopomer Abundances, *Appl. Environ. Microbiol.*, *72*(1), 638–644, doi:10.1128/AEM.72.1.638.

Tan, X., D. Shao, and W. Gu (2018), Effects of temperature and soil moisture on gross nitrification and denitrification rates of a Chinese lowland paddy field soil, *Paddy Water Environ.*, *16*(4), 687–698, doi:10.1007/s10333-018-0660-0.

Taylor, A. E., A. T. Giguere, C. M. Zoebelein, D. D. Myrold, and P. J. Bottomley (2017), Modeling of soil nitrification responses to temperature reveals thermodynamic differences between ammonia-oxidizing activity of archaea and bacteria, *ISME J.*, *11*(4), 896–908, doi:10.1038/ismej.2016.179.

Thilakarathna, S. K., and G. Hernandez-Ramirez (2021), Primings of soil organic matter and denitrification mediate the effects of moisture on nitrous oxide production, *Soil Biol. Biochem.*, *155*(February), 108166, doi:10.1016/j.soilbio.2021.108166.

Toyoda, S., H. Mutobe, H. Yamagishi, N. Yoshida, and Y. Tanji (2005), Fractionation of N2O isotopomers during production by denitrifier, *Soil Biol. Biochem.*, *37*(8), 1535–1545, doi:10.1016/j.soilbio.2005.01.009.

Toyoda, S., N. Yoshida, and K. Koba (2015), Isotopocule analysis of biologically produced nitrous oxide in various environments, *Mass Spectrom. Rev.*, *36*, 135–160, doi:10.1002/mas.

Van Groenigen, J. W., D. Huygens, P. Boeckx, T. W. Kuyper, I. M. Lubbers, T. Rütting, and P. M. Groffman (2015), The soil n cycle: New insights and key challenges, *Soil*, *1*(1), 235–256, doi:10.5194/soil-1-235-2015.

Vieten, B., T. Blunier, A. Neftel, C. Alewell, and F. Conen (2007), Fractionation factors for stable isotopes of N and O during N2O reduction in soil depend on reaction rate constant, *Rapid Commun. Mass Spectrom.*, *21*, 846–850, doi:10.1002/rcm.2915.

Wagner-Riddle, C., Q. C. Hu, E. van Bochove, and S. Jayasundara (2008), Linking Nitrous Oxide Flux During Spring Thaw to Nitrate Denitrification in the Soil Profile, *Soil Sci. Soc. Am. J.*, *72*(4), 908–916, doi:10.2136/sssaj2007.0353.

Well, R., I. Kurganova, V. L. De Gerenyu, and H. Flessa (2006), Isotopomer signatures of soil-emitted N2O under different moisture conditions - A microcosm study with arable loess soil, *Soil Biol. Biochem.*, *38*(9), 2923–2933, doi:10.1016/j.soilbio.2006.05.003.

Wen, Y., Z. Chen, M. Dannenmann, A. Carminati, G. Willibald, R. Kiese, B. Wolf, E. Veldkamp, K. Butterbach-Bahl, and M. D. Corre (2016), Disentangling gross N2O production and consumption in soil, *Sci. Rep.*, *6*(October), 1–8, doi:10.1038/srep36517.

Wenk, C. B. et al. (2016), Differential N2O dynamics in two oxygen-deficient lake basins revealed by stable isotope and isotopomer distributions, *Limnol. Oceanogr.*, *61*(5), 1735–1749, doi:10.1002/lno.10329.

Wrage, N., J. Lauf, A. del Prado, M. Pinto, S. Pietrzak, S. Yamulki, O. Oenema, and G. Gebauer (2004), Distinguishing sources of N2O in European grasslands by stable isotope analysis, *Rapid Commun. Mass Spectrom.*, *18*(11), 1201–1207, doi:10.1002/rcm.1461.

Wrage-Mönnig, N., M. A. Horn, R. Well, C. Müller, G. Velthof, and O. Oenema (2018), The role of nitrifier denitrification in the production of nitrous oxide revisited, *Soil Biol. Biochem.*, *123*(April), A3–A16, doi:10.1016/j.soilbio.2018.03.020.

Wong, W. W., M. F. Lehmann, T. Kuhn, C. Frame, S. C. Poh, I. Cartwright, and P. L. M. Cook (2020), Nitrogen and oxygen isotopomeric constraints on the sources of nitrous oxide and the role of submarine groundwater discharge in a temperate eutrophic salt-wedge estuary, , 1–15, doi:10.1002/lno.11664.

Wu, D., J. R. Köster, L. M. Cárdenas, N. Brüggemann, D. Lewicka-Szczebak, and R. Bol (2016), N2O source partitioning in soils using 15N site preference values corrected for the N2O reduction effect, *Rapid Commun. Mass Spectrom.*, *30*(5), 620–626, doi:10.1002/rcm.7493.

Wu, D., L. M. Cárdenas, S. Calvet, N. Brüggemann, N. Loick, S. Liu, and R. Bol (2017), The effect of nitrification inhibitor on N2O, NO and N2 emissions under different soil moisture levels in a permanent grassland soil, *Soil Biol. Biochem.*, *113*, 153–160, doi:10.1016/j.soilbio.2017.06.007.

Wu, D., R. Well, L. M. Cárdenas, R. Fuß, D. Lewicka-Szczebak, J. R. Köster, N. Brüggemann, and R. Bol (2019), Quantifying N2O reduction to N2 during denitrification in soils via isotopic mapping approach: Model evaluation and uncertainty analysis, *Environ. Res.*, *179*(August), doi:10.1016/j.envres.2019.108806.

Xia, Z., H. Xu, G. Chen, D. Dong, E. Bai, and L. Luo (2013), Soil N2O production and the δ15N-N2O value: Their relationship with nitrifying/denitrifying bacteria and archaea during a growing season of soybean in northeast China, *Eur. J. Soil Biol.*, *58*, 73–80, doi:10.1016/j.ejsobi.2013.05.008.

Yamamoto, A., H. Akiyama, Y. Nakajima, and Y. T. Hoshino (2017), Estimate of bacterial and fungal N2O production processes after crop residue input and fertilizer application to an agricultural field by15N isotopomer analysis, *Soil Biol. Biochem.*, *108*, 9–16, doi:10.1016/j.soilbio.2017.01.015.

Yang, H., H. Gandhi, N. E. Ostrom, and E. L. Hegg (2014), Isotopic fractionation by a fungal P450 nitric oxide reductase during the production of N2O, *Environ. Sci. Technol.*, *48*(18), 10707–10715, doi:10.1021/es501912d.

Yu, L. et al. (2020), What can we learn from N2O isotope data? − Analytics, processes and modelling , *Rapid Commun. Mass Spectrom.*, (June), 1–14, doi:10.1002/rcm.8858.

Yoshida, N., and S. Toyoda (2000), Constraining the atmospheric N2O budget from intramolecular site preference in N2O isotopomers, *Nature*, *405*(6784), 330–4, doi:10.1038/35012558.

Zeglin, L. H., P. J. Bottomley, A. Jumpponen, C. W. Rice, M. Arango, A. Lindsley, A. McGowan, P. Mfombep, and D. D. Myrold (2013), Altered precipitation regime affects the function and composition of soil microbial communities on multiple time scales, *Ecology*, *94*(10), 2334–2345, doi:10.1890/12-2018.1.

Zhang, J., T. Lan, C. Müller, and Z. Cai (2015), Dissimilatory nitrate reduction to ammonium (DNRA) plays an important role in soil nitrogen conservation in neutral and alkaline but not acidic rice soil, *J. Soils Sediments*, *15*(3), 523–531, doi:10.1007/s11368-014-1037-7.

Zhang, W., Y. Li, C. Xu, Q. Li, and W. Lin (2016), Isotope signatures of N 2 O emitted from vegetable soil: Ammonia oxidation drives N 2 O production in NH 4+-fertilized soil of North China, *Sci. Rep.*, *6*(April), 1–10, doi:10.1038/srep29257.

Zhang, H., and K. Yemoto (2018), UAS-based remote sensing applications on the Northern Colorado Limited Irrigation Research Farm, *Int. J. Precis. Agric. Aviat.*, *1*(1), 1–10, doi:10.33440/j.ijpaa.20190202.50.

References From the Supporting Information

Hu, H. W., D. Chen, and J. Z. He (2015), Microbial regulation of terrestrial nitrous oxide formation: Understanding the biological pathways for prediction of emission rates, *FEMS Microbiol. Rev.*, *39*(5), 729–749, doi:10.1093/femsre/fuv021.

Stuchiner, E. R., Z. D. Weller, and J. C. Fischer (2020), An approach for calibrating laser−based N 2 O isotopic analyzers for soil biogeochemistry research , *Rapid Commun. Mass Spectrom.*, (June 2020), 1–14, doi:10.1002/rcm.8978.